Two-Tank MultiCompartment Redox Flow Battery

Luisa C. Brée[1], Alexander Mitsos[2,1,3]*

[1] *Process Systems Engineering (AVT.SVT), RWTH Aachen University, 52074 Aachen, Germany*

[2] *JARA-ENERGY, 52056 Aachen, Germany*

[3] *Energy Systems Engineering (IEK-10), Forschungszentrum Jülich, 52425 Jülich, Germany*

Keywords:

Redox Flow Battery

Roundtrip Efficiency

Depth of Discharge

Investment Costs

Abstract: We propose novel designs and operation strategies for redox flow batteries with the aim of higher roundtrip efficiencies (electric to chemical to electric) together with decreased amount of electrolyte. Such new designs are based on additional electrolyte tanks and compartmentalized electrodes. We analyze roundtrip efficiencies for these designs utilizing charge and discharge curves for different current densities. For commonly applied operating conditions, the results indicate that the proposed modifications and their combination result in slightly lower amount of required electrolyte and marginally higher roundtrip efficiencies as the state of the art. However, if higher per pass changes are envisaged, the savings are more significant (up to 4% higher roundtrip efficiency). A change in roundtrip efficiency has an impact on operating costs. Possible reductions in operating costs have to be contrasted with any additional investment costs and are therefore considered cumulatively as total costs. The results indicate that if higher per pass changes are envisaged, additional electrolyte tanks for setting up a two tank configuration are economically beneficial.

Corresponding author: *A. Mitsos
AVT Process Systems Engineering, RWTH Aachen University, 52074 Aachen, Germany
E-mail: amitsos@alum.mit.edu

1 Introduction

Electrochemical energy storage systems directly convert electrical energy into chemical energy and back. Since they also lead to relatively high roundtrip efficiency, they are well suited for the storage of electricity from fluctuating renewable energy sources. The redox flow battery (RFB) is particularly promising for large-scale storage, because the energy storage capacity is characterized by the electrolyte volume and respective concentration, whereas the rated power is characterized by the reactive electrode area. Thus they are independently scalable in contrast to conventional batteries[6]. Of the several existing redox flow battery chemistries, the vanadium redox flow battery (VRFB) is the most mature and some VRFB systems have been successfully demonstrated at megawatt scale[15]. For instance, a 200MW/800MWh vanadium flow battery is under construction in Dalian, China[20].

The VRFB stores energy by using vanadium redox couples (V2+/V3+ and V4+/V5+) in two electrolyte tanks, one per halfcell. VRFBs exploit the four oxidation states of vanadium allowing a single active element in both anolyte and catholyte[5]. During the charge/discharge cycles, H^+-ions are exchanged through the ion-selective membrane. According to Chakrabarti et al.[6], charge or discharge efficiency can be as high as 85%, VRFBs have a fast response time, a lifetime of $>$ 10 years and can operate for 5,000 - 14,000 cycles. The Electric Power Research Institute gives similar values with a response time of microseconds from zero output to full output if the cells are filled with electrolyte, a lifetime of 10-15 years with 1,000 (dis-)charge-cycles per year[7].

However, market penetration of the VRFB for large-scale energy storage is limited by the high capital cost, which largely results from the low energy density of the vanadium redox couples (according to Alotto et al.[3], the stored energy density does not exceed 25-35 Wh/L) and the high vanadium purchase costs[15]. This makes a reduction of the required amount of electrolyte necessary.

High roundtrip efficiency is crucial for energy storage. For VRFB's different

approaches to increase efficiency are being pursued in literature including improvement of employed materials[16] or electrolyte flowrates[2]. We propose novel designs and operation strategies aiming at the improvement of roundtrip efficiency and reduced use of electrolyte. In future work, the design proposed here could also be combined with a variable electrolyte flowrate that is optimized to current State of Charge (SOC) of the VRFB possibly achieving even higher efficiencies.

The state of the art configuration of a RFB is equipped with one electrolyte storage tank for each halfcell (Figure 1, upper left). We call this design OneTank-configuration (OT). The electrolyte is pumped through the electrochemical cells several times in order to be (dis-)charged as the SOC is changed by ΔSOC per pass through the cell. The amount of currently stored energy is characterized by the SOC of the electrolyte. Usually the batteries are built in form of stacks having several electrochemical cells in parallel as shown in the Figure.

In the state of the art configuration, the stream exiting the electrode is mixed with the electrolyte tank content. This results in exergy destruction which is thermodynamically not favorable. Recently, concurrently with our calculations, Liu et al. suggested a no-mixing design of a VRFB to overcome this exergy destruction[10]. Likewise, we propose to use two tanks for each electrolyte: one for the "charged" state and one for the "discharged", i.e., instead of the SOC as a property of the electrolyte (essentially the concentration of "charged" material), we have the SOC as the filled portion of the tanks. We call this configuration TwoTank (TT) (Figure 1, upper right). In the TwoTank configuration, there is no mixing with uncharged electrolyte. The elimination of exergy destruction in principle can lead to higher efficiency. In thermal energy storage (e.g., molten salt storage in concentrated solar power) two tank systems are standard and known to have substantially higher efficiency[14]. As ΔSOC in VRFBs typically is small with values around $\sim 3-4\%$, the TwoTank concept has to be extended by allowing multiple passes of the fluid through the reactor through an intermediate

small tank or through batches for using the whole usable range of SOC. Like Liu et al.[10], we analyze the latter idea and assume that once a tank is emptied, the other tank of that halfcell now is the source of electrolyte and the tank that is empty at this moment then is the sink. This is depicted by the dotted arrows in Figure 1. Note that the rather small per pass change of charge implies that the exergy destruction is not dramatic in the OneTank configuration. This is in contrast to thermal energy storage, wherein large temperature differences (>100K) are used[4;11].

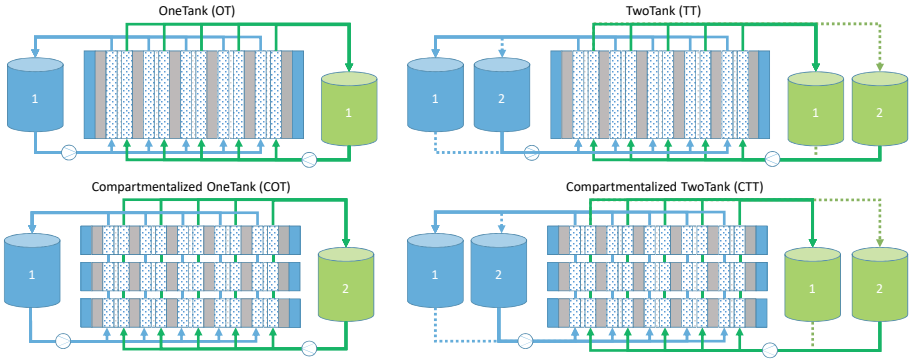

Fig. 1: Scheme of the different design configurations for a VRFB under investigation in this study considering additional tanks or compartmentalization. The OT configuration represents the state of the art.

Not considered by Liu et al.[10] in the analysis of their no-mixing design is a second challenge of electrochemical systems with flow (fuel cell, electrolytic reactors, redox flow battery), which is that the concentration changes along the flow direction. This concentration gradient implies that the open circuit potential (OCV), which is the reversible limit, and the required voltage (for given transport resistances) changes along the flow direction. However, the electrodes are good electrical conductors so that the voltage is spatially nearly uniform. Therefore, the most disadvantageous voltage is always applied over the entire flow direction (the highest voltage when charging, the lowest when discharging) which results in further losses. Again, the higher the change in SOC per pass (ΔSOC), the higher the losses, as the difference between total cell potential and OCV is even higher at the inlet during charge and at the outlet during

discharge. Moreover, the impact of spatially uniform voltage on energy losses becomes higher towards the bounds of the SOC (close to 0% and 100%) where the derivative of the voltage curve has a high absolute value (see also Figure 5) and thus the losses highly depend on ΔSOC. Avoiding the high losses at the bounds of SOC, is one reason why in industrial applications the battery is never fully charged or discharged. Another reason for limiting the upper bound of SOC is that operation at above ∼80% SOC may result in undesired reactions. For instance, the Electric Power Research Institute (EPRI) reports the electrolysis of water into hydrogen on the negative electrode and oxygen at the positive at high voltages (called overcharge)[7]. These undesired side-reactions occur in aqueous electrolytes. The use of non-aqueous electrolytes allows the operation at higher voltages[8;17], however, they are not used at industrial scale[17]. EPRI states that the VRFB, however, tolerates over-discharge, which is the voltage decrease towards the lower bound in SOC[7].

The Depth of Discharge (DOD) takes into account the fact that the usable state of charge (SOC) often is limited in reality[19] among others due to the reasons mentioned above. DOD is the difference of upper bound (SOC_{ub}) and lower bound (SOC_{lb}) of state of charge applied in the operation:

$$\mathrm{DOD} = \mathrm{SOC}_{ub} - \mathrm{SOC}_{lb}.$$

A direct consequence of small DOD is that a substantial amount of the electrolyte can not be used for storing energy. E.g., compared to full use of 0...100%, the electrolyte's working range 25...75% requires double the electrolyte material (simplistically assuming constant efficiency). This also implies higher investment costs for the surplus of electrolyte material and larger installed tanks to fit the surplus electrolyte. As already stated above, electrolyte material is expensive.

In current state of the art RFB systems, losses due to the spatially uniform voltage being applied over the entire flow direction are small if ΔSOC is kept

small. In order to allow higher ΔSOC's but keep losses low, we suggest to divide the electrode into multiple compartments in series. This allows to apply a different voltage to each compartment. We call this configuration compartmentalized OneTank (COT) (Figure 1, lower left). Therefore, compartmentalization seems important if high total differences in SOC are used. This idea is complementary to the TwoTank configuration. In other words, we allow for both TT and COT adjustments in the compartmentalized TwoTank configuration (COT).

The proposed design modifications aim at overcoming both issues of exergy destruction due to mixing in a single tank and due to a unique voltage along the flow direction and as such should result in higher efficiency, especially for full cycles (0...100% SOC).

We set up a model in order to calculate the roundtrip efficiencies of all configurations. A subsequent cost analysis takes into account investment costs and operating cost differences for the configurations in order to reveal the most beneficial setup.

2 Roundtrip Efficiency

The roundtrip efficiencies for all above presented configurations are analyzed. For this purpose, a model is introduced in the first part of this section which is subsequently used to compare the roundtrip efficiencies based on voltage curves.

2.1 Modeling

We assume that no side reactions occur, the electrolyte in the cell and tank is perfectly mixed and the electrolyte volume in each half-cell is constant (i.e. there is no crossover of active species through the membrane). The roundtrip efficiency ε is calculated by the ratio of electrical energy available when discharging W_{out} and electrical energy needed for charging W_{in}. This is equal to the power integral for discharge over DOD divided by the power integral for

charge over the inverted DOD (1).

$$\varepsilon = \frac{W_{out}}{W_{in}} = \frac{\int_{\mathrm{SOC}_{ub}}^{\mathrm{SOC}_{lb}} P_{discharge}\mathrm{dSOC}}{\int_{\mathrm{SOC}_{lb}}^{\mathrm{SOC}_{ub}} P_{charge}\mathrm{dSOC}} \tag{1}$$

$$\Rightarrow \varepsilon \overset{\frac{dI}{dt}=0}{=} \frac{\int_{\mathrm{SOC}_{ub}}^{\mathrm{SOC}_{lb}} U_{discharge}\mathrm{dSOC}}{\int_{\mathrm{SOC}_{lb}}^{\mathrm{SOC}_{ub}} U_{charge}\mathrm{dSOC}} \tag{2}$$

Typically, a RFB is operated at a current I that is fixed to the same value for charging and discharging. Then, ε can equivalently be calculated by the ratio of the voltage integrals (2). The cell voltage while charging and discharging depends on the SOC of the RFB as shown in Figure 5. Therefore, the area beneath the respective curve within DOD represents the amount of electricity used to charge the RFB and discharged from the RFB. Since in reality the worst voltage is always applied along the entire flow direction and the SOC of the electrolyte is changed by ΔSOC at each cell passage, the required/released electricity is determined by the area resulting from the multiplication of the worst voltage and ΔSOC, as depicted in Figure 2. Therefore, we calculate the voltage integrals for ε by the summation of the voltages corresponding to the current SOC of the electrolyte leaving the cell (or compartment) $U(\mathrm{SOC}_{out})$ multiplied with ΔSOC (3).

$$\Rightarrow \varepsilon = \frac{\sum^{\mathrm{DOD}} U_{discharge} \cdot \Delta\mathrm{SOC}}{\sum^{\mathrm{DOD}} U_{charge} \cdot \Delta\mathrm{SOC}} \tag{3}$$

$$U_{discharge} = f(\mathrm{SOC}_{out})$$

$$U_{charge} = f(\mathrm{SOC}_{out})$$

One pass of electrolyte through the cell with change in SOC is depicted in Figure 2 (left). $U(\mathrm{SOC})$ is a continuous function of SOC, however, the most disadvantageous voltage (which is $U(\mathrm{SOC}_{out})$) has to be applied to the cell. If the stack is compartmentalized into two compartments where both compartments are characterized by a halved value in ΔSOC, different voltages may be applied to the compartments (see Figure 2, right) while the total change in SOC after

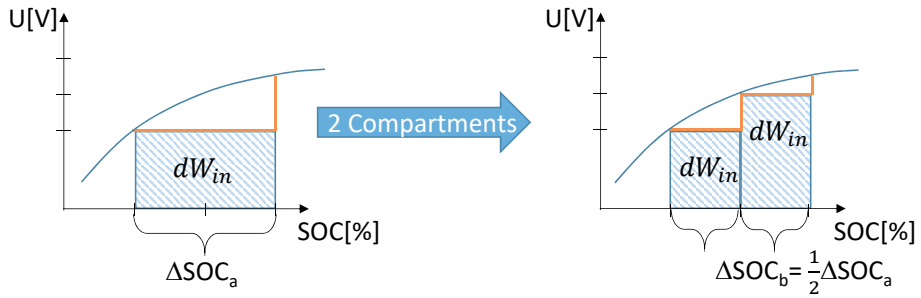

Fig. 2: Illustration of compartmentalization effect on voltage. Left part shows single-compartment, right two compartments. The halving of ΔSOC from left to right due to compartmentalization results in reducing the integral of the voltage (corresponding to efficiency).

leaving the cell is equal to ΔSOC of the non-compartmentalized cell. Then, the losses of the compartmentalized cell are lower which we will show in Section . In Figure 3 the change in SOC and $U(\mathrm{SOC}_{out})$ is presented for each configuration. It visualizes that for OneTank configurations, the SOC of the passing electrolyte is increased to a higher value (e.g., from $\mathrm{SOC}_{in,P1}$ to $\mathrm{SOC}_{out,P1}$ in the first pass). This, however, results after mixing in a SOC of the electrolyte of $\mathrm{SOC}_{in,P2}$ which again will be changed by ΔSOC to $\mathrm{SOC}_{out,P2}$ in the second pass. In the TwoTank configurations, the SOC of the passing electrolyte is also increased to a higher value (e.g. from $\mathrm{SOC}_{in,P1}$ to $\mathrm{SOC}_{out,P1}$ in the first pass). As there is no mixing with electrolyte at a lower SOC, once all the electrolyte is at $\mathrm{SOC}_{out,P1}$, the next pass will be carried out from $\mathrm{SOC}_{in,P2}$ to $\mathrm{SOC}_{out,P2}$. Compartmentalization divides the increase of SOC into smaller steps.

Taking a closer look at the different operating strategies, we will describe the established model in the following. In the OneTank configuration, a small portion of the electrolyte is pumped through the cell. In this portion, the concentration of the ions c_i is electrochemically changed which results in a changed composition of the tank content after mixing. The concentration of the electrolyte volume in the tank therefore changes according to eq. (4) based on the assumption of an ideally mixed tank. It depends on the total electrolyte volume V_{Tank} and the electrolyte volume pumped through the cells per cycle V_{pass}. M_i

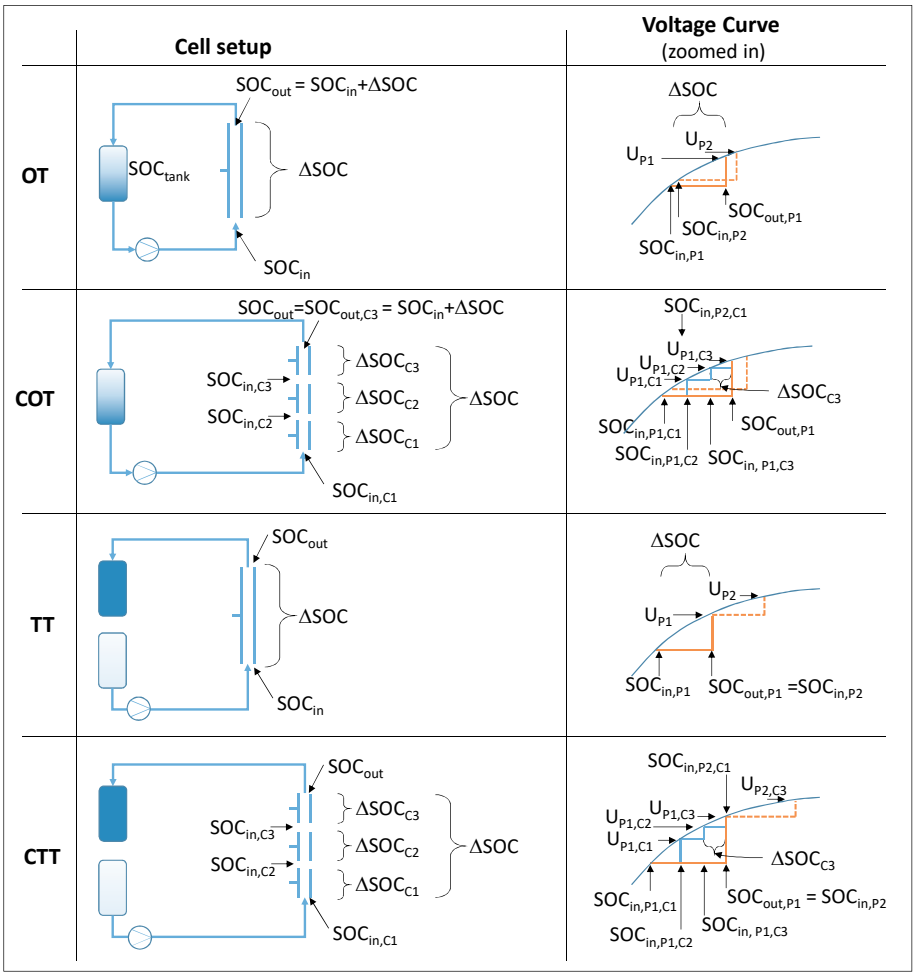

Fig. 3: Comparison of the different configurations: Left column shows the setup of each configuration and the variable's naming. Right column shows stepwise voltage increase with SOC in each configuration for two passes (Potential curve is zoomed in. The passes are indicated via subscripts P1 for first pass and P2 for second pass).

is the molar mass of each ion. In eq. (5) c_i is exchanged by SOC_Tank as this is the representation of the concentration of the charged species in the tank.

$$V_{\mathrm{Tank}} M_i \frac{dc_{i,\mathrm{Tank}}}{dt} = (c_{i,\mathrm{Tank,in}} - c_{i,\mathrm{Tank,out}}) M_i \dot{V}_{\mathrm{pass}} \tag{4}$$

$$V_{\mathrm{Tank}} \frac{d\mathrm{SOC}_{\mathrm{Tank}}}{dt} = \underbrace{(\mathrm{SOC}_{\mathrm{Tank,in}} - \mathrm{SOC}_{\mathrm{Tank,out}})}_{\Delta\mathrm{SOC}} \dot{V}_{\mathrm{pass}} \tag{5}$$

This means that in the case of the OneTank configurations for reaching SOC_{ub} in the total electrolyte tank, the exiting SOC of the electrolyte has to be even higher than SOC_{ub}. Discretization of eq. (5) with respect to time results in

$$\mathrm{SOC}_{\mathrm{Tank,new}} = \frac{\mathrm{SOC}_{\mathrm{Tank,old}} \cdot V_{\mathrm{Tank}} + \Delta\mathrm{SOC} \cdot V_{\mathrm{pass}}}{V_{\mathrm{Tank}}}. \tag{6}$$

The resulting change in SOC of the total electrolyte volume in the tank $\mathrm{SOC}_{\mathrm{Tank}}$ is smaller than ΔSOC. The electrolyte passes through the cell are indicated via subscripts P (see also in Figure 3). Applying this nomenclature to the equation for two passes (P1 for first pass and P2 for second pass), we replace $\mathrm{SOC}_{\mathrm{Tank,old}}$ in (6) by $\mathrm{SOC}_{\mathrm{Tank,P1}}$ and $\mathrm{SOC}_{\mathrm{Tank,new}}$ by $\mathrm{SOC}_{\mathrm{Tank,P2}}$.

When the cell is divided into multiple compartments, the total change ΔSOC in a compartmentalized setup is equal to the sum of changes in SOC over all compartments n_{c}

$$\Delta\mathrm{SOC} = \sum_{c=1}^{n_c} \Delta\mathrm{SOC}_{\mathrm{c}} \tag{7}$$

where the SOC of the passing electrolyte is changed in every compartment by $\Delta\mathrm{SOC}_c$. The SOC of the electrolyte leaving one compartment is calculated via

$$\mathrm{SOC}_{\mathrm{out,c}} = \mathrm{SOC}_{\mathrm{in,c}} + \Delta\mathrm{SOC}_{\mathrm{c}} \tag{8}$$

where $\mathrm{SOC}_{\mathrm{in,c}}$ is the SOC of the passing electrolyte being pumped into the compartment c and $\mathrm{SOC}_{\mathrm{out,c}}$ the SOC of the electrolyte leaving that compartment c. The SOC can by definition not exceed 100% or be lower than 0%. Therefore, the combination of DOD and $\Delta\mathrm{SOC}_{\mathrm{c}}$ is limited by (8).

The voltages for charging and discharging are evaluated at every outlet of the compartments and summed up to the total voltage

$$U_{\text{tot,charge/discharge}} = \sum_{1}^{nc} U(\text{SOC}_{\text{out,c}}).$$

In the case of TwoTank, V_{Pass} in the model is set to V_{Tank}. This is valid, as the concentrations at the inlet are the same for the whole electrolyte volume for one batch, i.e., until all of the electrolyte has been pumped through the electrochemical cell. With this assumption (6) simplifies to $\text{SOC}_{\text{Tank,new}} = \text{SOC}_{\text{Tank,old}} + \Delta\text{SOC}$ (or $\text{SOC}_{\text{Tank, P2}} = \text{SOC}_{\text{Tank,P1}} + \Delta\text{SOC}$ for two passes).

The potential at charge or discharge depends on the applied current density, the concentrations of the involved species and on the material components via occurring overpotentials. In order to calculate the potential at each SOC, an electrochemical model was set up based on widely known equations as, e.g., given in Minke et al.[12]: The total cell voltage U_{cell} can be described as the sum of the equilibrium voltage E_0 and the overpotentials η. We use the concentration-dependent equilibrium potential for each electrochemical reaction calculated by the Nernst equation[13].

The overpotentials are summarized in a cumulated loss term. With this approach we account for overpotentials in the calculation of the voltage curves arising through, e.g., ohmic losses or phenomena such as limited charge or mass transfer without explicitly modeling these effects. For details on modelling of such phenomena many publications exist. For instance, Wei et al. present both a mechanistic model[23] and models with first order resistance-capacitance models to represent the dynamic behaviour in the electrochemical process of the considered VRFB via electrical analogy[22;21]. In order to have realistic values for the cumulated loss term, we use a value from Minke et al.[12], who report the sum of all overpotentials for the also herein considered cell as $0.072\text{k}\Omega\text{m}^2$ for SOC=0.5 in a system with initial vanadium concentration of 1.6 mol/l and a sulfate concentration of 4 mol/l. In order to capture the limits of mass trans-

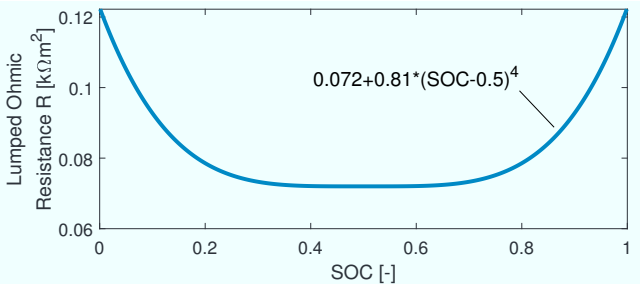

Fig. 4: Lumped ohmic resistance over SOC including concentration overpotential.

port at the boundaries of the SOC we modify the lumped ohmic resistance such that the resistance increases at the edges. The course of the curve at the edges remains subject to a high degree of uncertainty as the magnitude and slope require experimental validation. A steeper slope at the edges would increase the impact of the herein considered design and operational changes on efficiency, a lower slope would mitigate the positive effect of the changes. Figure 4 presents the herein assumed course of the lumped ohmic resistance over the SOC range with the value taken from literature at SOC=0.5. The calculated voltage curves are shown in Figure 5 for the ideal case and for charge and discharge at $j = 200\text{mA/cm}^2$. In the ideal case no electric current is applied so that the equilibrium voltage corresponds to the OCV of the cell. The calculated ideal curve is identical to the curve presented in Minke et al.[12].

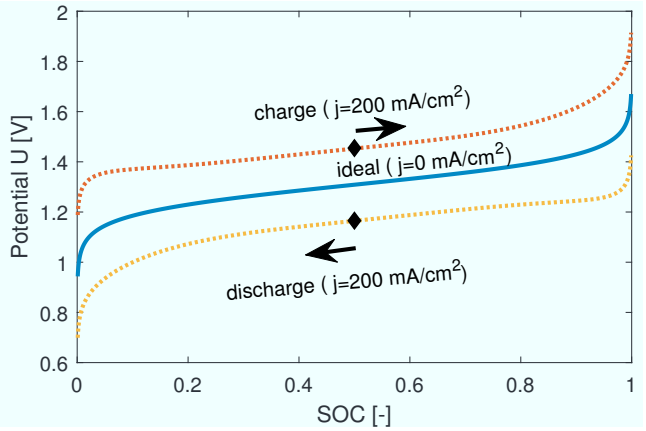

Fig. 5: Voltage curves plotted within SOC $\in [0.001, 0.999]$ at j=0mA/cm^2 and j=200mA/cm^2 for a VRFB with initial vanadium concentration of 1.6 mol/l, a sulfate concentration of 4 mol/l and the lumped ohmic resistance given in Figure 4. ◆ presents data of Minke et al.[12] for the system at j=200mA/cm^2. The calculated ideal curve is identical to the curve presented in Minke et al.[12].

Note that a change in V_{pass}, V_{Tank} or their ratio only has an influence on the absolute value of $U_{\text{tot,discharge}}$ and $U_{\text{tot,charge}}$. The ratio of the two potentials, which is equal to the roundtrip efficiency, however, remains the same as ΔSOC is fixed. Rewriting eq. (6) into its differential form

$$\frac{d\text{SOC}_{Tank}}{dt} = \frac{V_{pass}}{V_{Tank}}\Delta\text{SOC}$$

reveals the linearly proportional influence on SOC_{Tank} for charge and discharge equally.

2.2 Efficiency-Comparison

Roundtrip efficiency of all configurations will be analyzed based on varying DOD, ΔSOC and current densities in four different scenarios introduced in Table 1. Scenario 1 and 2 represent typical operating ranges of SOC (20...80% in Scenario 1 and 10...90% in Scenario 2) with a typical ΔSOC of 3.5%. We

define the reference case as the OT-configuration operated according to Scenario 2. Scenario 3 broadens the DOD, resulting in lower roundtrip efficiencies. However, the broadened SOC reduces the necessary volume of electrolyte as the electrolyte at hand is charged and discharged to higher and lower SOC's, respectively. Scenario 4 introduces a change in ΔSOC. This could be realized by lower pumping rates of the electrolyte through the cell. In Scenario 3, going to such high and low SOC's, problems may arise due to temperature management or electrolyte imbalance. For instance, in aqueous electrolytes side reactions can occur at elevated SOCs producing gases[7]. This results in a reduced coulombic efficiency and, even more important for cell capacity, according to Tang et al. the possible imbalance between the SOCs of the two electrolytes if the gas reactions do not take place to the same extent in both half cells[18]. In particular, the evolution of hydrogen at the negative electrode may start earlier (already at $\geqslant$ 90% SOC) than the oxygen evolution at the positive electrode. However, the use of non-aqueous electrolytes allows the operation at higher voltages[8;17] but may require elevated investment costs.

In particular, in aqueous electrolytes, the evolution of hydrogen at the negative electrode may start earlier (already at $\geqslant$90% SOC) than the oxygen evolution at the positive electrode.

In the following calculations we consider the results at three different current densities: $j = 0, 80$ and 200 mA/cm^2. The typical operating current density of VRFBs is 80 mA/cm^2 according to Weydanz et al.[24] or $50-80$ mA/cm^2 as given by Kim et al.[9], and stored energy density is according to Kim et al.[9] in the range of $25-35$ Wh/L or $20-32$ Wh/kg. The current density of $j = 200$ mA/cm^2 was chosen, as it was already taken by Minke et al.[12] for the cell under investigation, which is the same as we focus on in our study, for industrial application. Within our study, the current densities are applied to all configurations in our roundtrip efficiency calculations. In future work, the current density may be optimized for each configuration, for each compartment in the compartmentalized designs and also for each SOC in order to achieve even higher roundtrip efficiencies.

Table 1: Scenarios

	Scenario 1	Scenario 2	Scenario 3	Scenario 4
SOC_{lb} [%]	20	10	4.5	10
SOC_{ub} [%]	80	90	95.5	90
ΔSOC [%]	3.5	3.5	3.5	9

We consider charging first, starting from the lower bound of the SOC (SOC_{lb}) until the upper bound of SOC (SOC_{ub}) is reached. Once the SOC is higher or equal to SOC_{ub}, the discharge process is calculated starting from the lastly calculated SOC_{up} to reach a value smaller or equal to SOC_{lb}.

For reaching SOC_{ub} in the total electrolyte tank in the case of the OneTank configurations, the SOC of the electrolyte that exits the cell has to be even higher than SOC_{ub} (see eq. (4) and Figure 3). But, if SOC_{ub} is close to the limit of 100% and if the SOC at the inlet is already highly charged, the SOC of the passing electrolyte can only be charged up to its physical limit. The ΔSOC then is smaller than the desired operating choice, as these upper and lower bounds in SOC can not be exceeded. Theoretically the physical limits for SOC are 0% and 100%. In our calculations we set these limits to 0.001% and 99.99%, as towards the limits of SOC, the potential goes towards infinity and the utilized Nernst equation does not give meaningful results. The scenarios are chosen such that the limits are not reached during the cycles.

Figure 6 presents the roundtrip efficiencies for all configurations for the scenarios introduced in Table 1. Currently, $V_{pass} = 0.01 \cdot V_{tank}$ is assumed. Furthermore, W_{out} is kept fix. This is the most realistic case and has interesting implications. If a configuration CON has a better roundtrip efficiency than the state of the art, plant size of configuration CON may be lower if W_{out} is fixed. Then, the size of configuration CON may be lower than that of OT by the

efficiency ratio $\Delta\varepsilon$ according to

$$\Delta\varepsilon_{CON,\mathrm{OT}} = 1 - \frac{W_{in,CON}}{W_{in,\mathrm{OT}}} = 1 - \frac{\frac{W_{out}}{\varepsilon_{CON}}}{\frac{W_{out}}{\varepsilon_{\mathrm{OT}}}} = 1 - \frac{\varepsilon_{CON}}{\varepsilon_{\mathrm{OT}}}. \tag{9}$$

If the investment costs are linearly proportional to W_{in}, also the investment costs of configuration CON are lower by $\Delta\varepsilon$.

$\Delta\varepsilon_{CON,\mathrm{OT}}$ is calculated for every modification compared to the efficiency of the state of the art $\varepsilon_{\mathrm{OT}}$ in the same scenario and is given in Figure 6. Also given in that figure is the efficiency ratio $\Delta\varepsilon_{CON,\text{OT-Scen2}}$ which is based on the efficiency ratio with respect to OT in the scenario with the typically applied operation, i.e., Scenario 2.

In all scenarios the configurations can be ranked according to their roundtrip efficiency in the same descending order: CTT>TT>COT>OT. TwoTank configurations are therefore better than OneTank configurations, and Compartmentalization is better than no Compartmentalization.

The efficiencies in Scenarios 1 and 2 are very similar for all investigated current densities for each respective configuration, only slightly lower for the broader SOC-range in Scenario 2.

Increasing DOD from 10...90% in Scenario 2 to 4.5...95.5% in Scenario 3 again leads to slightly lower roundtrip efficiencies in each configuration, respectively, due to steeper U-curves at the bounds in SOC. However, with the herein chosen U-Curves, the effect is small. A lower roundtrip efficiency leads to higher energy losses. An increase in DOD and thus decrease in roundtrip efficiency might nonetheless be reasonable as less electrolyte and less tank volume needs to be acquired. This is why a subsequent analysis of the investment costs is conducted in Section3.

If ΔSOC is large with 9% in Scenario 4, the roundtrip efficiencies of both OneTank configurations (OT and COT) decrease significantly whereas the TwoTank configurations (TT and CTT) have only small reductions in roundtrip efficiency. Compared to the reference case (OT in Scenario 2), the roundtrip efficiency of

CTT is lower by only 0.5% whereas OT in this scenario is lower by 3.2% compared to its roundtrip efficiency when SOC is operated in the range 10...90% with ΔSOC=3.5%. Compared to OT in the same scenario, the roundtrip efficiency of CTT is better by 3.9%.

In the investigations of Liu et al.[10], where they analysed a TT configuration for a single-cell VRFB system with a halfcell volume of 35ml, they did not limit SOC, but fixed an upper and lower limit for the applied cell potential (to 1.7V and 0.8V, respectively). With this approach different upper and lower values of SOC were reached from which they calculated an electrolyte utilization rate. They found that the TT configuration increases the utilization rate by more than 10%. In our calculations, we do not allow for different utilization rates, but fix DOD. The voltage efficiency of the system analysed by Liu et al.[10] was increased by ∼2%. The efficiency increase in our system is lower than that of Liu et al., as the voltage curves of the small-scale system of Liu et al.[10] were characterized by higher losses especially during discharge already at values around 0.25 SOC where our assumed lumped ohmic resistance is still relatively small. However, especially for VRFBs at industrial scale, low losses are urgently required for energy storage to make any sense at all. Therefore, we think that it is also important to evaluate the suggested modifications with a more optimistic assumption of low losses in the voltage curve leading to more pessimistic results of the newly proposed modifications.

The results in Figure 6 indicate that configurations with compartmentalization (COT and CTT) are always more efficient than the same setup without compartmentalization (OT and TT) for the same scenario, respectively. However, the impact due to the installation of two tanks increases the roundtrip efficiency even more and the combination of both leads to the highest roundtrip efficiencies. The CTT configuration allows larger DOD and ΔSOC with only low efficiency losses compared to the current state of the art.

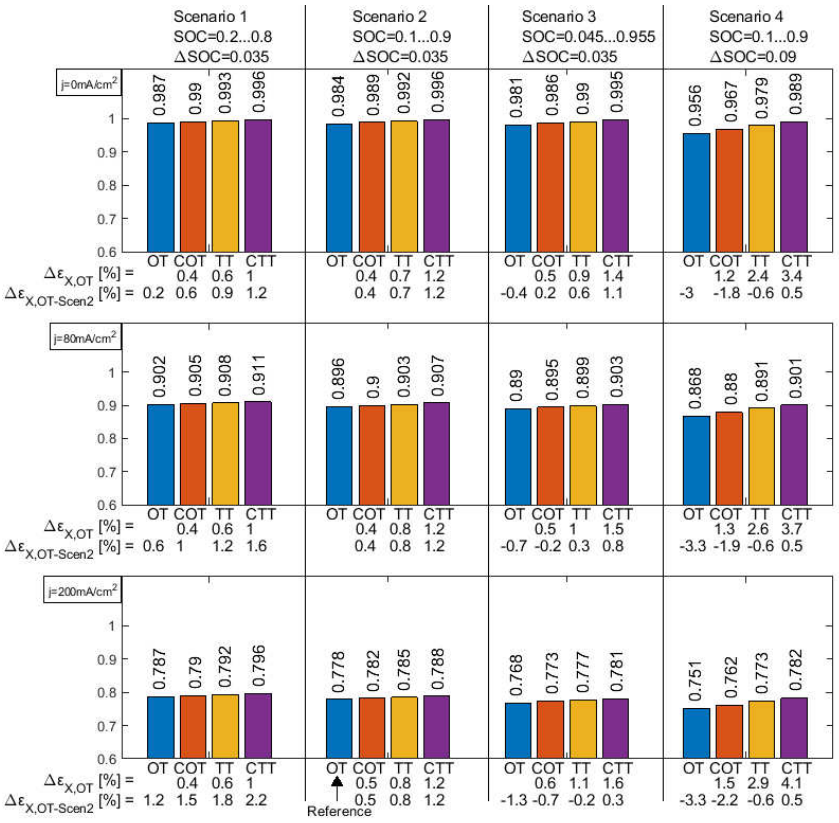

Fig. 6: Roundtrip efficiencies of the different configurations for the scenarios (columns) introduced in Table 1 and for different current densities (rows).

3 Cost Calculation

A higher roundtrip efficiency of a VRFB leads to lower need of electrolyte and lower energy input. However, for reaching the higher efficiencies presented above, further investments for additional tanks or compartments are required. The changes in investment costs and operating costs therefore have to be contrasted. In the following calculations we consider the efficiency results of $j = 200\text{mA/cm}^2$ as this current density was assumed in the original techno-economic model set up by Minke[12].

3.1 Investment Cost Calculation

In Minke[12] techno-economic modeling and analysis of stationary vanadium-redox-flow battery systems at industrial scale was conducted. According to Minke, the investment costs C_{Inv} can be divided into the costs for the rated power output of the battery C_{RP} and the costs for the energy storage $C_{storage}$ via

$$C_{Inv} = C_{storage} + C_{RP}.$$

The costs due to the rated power can again be divided into the costs of a stack C_{Stack} for the number of all stacks n_{Stacks} and the connection of the stacks C_C.

$$C_{RP} = n_{Stacks} \cdot C_{Stack} + C_C.$$

The costs of one stack are based on the component-costs of the the membranes C_M, electrodes $C_{Electrode}$, bipolar plates C_{BPP}, current collectors C_{CC}, cell framing C_{CF}, stack framing C_{SF} and assembly $C_{RP,Assembly}$. The component-costs depend on the specific component prices p (given in Table 2 in the Appendix) and hereafter described scale factors (see also equations (13)-(18) in the Appendix). The costs of the membranes depend on the number of cells n_{Cells} and the cross-sectional cell area A_C. The costs of the electrodes additionally have to be multiplied by 2, as each cell requires two electrodes. The bipolar

plates depend on the cross-sectional cell area and number of cells plus one. Two current collectors per stack, one cell framing per cell and one stack framing per stack are required, respectively.

The compartmentalization may require the division of the cells into compartments. As the cells are connected into stacks, these stacks need to be divided. The division of one stack, e.g., into two compartments, is equal to building a battery with two stacks. The number of cells in each stack remains the same. We assume that the cells in the compartmentalized stacks have half of the cross-sectional cell area as in the non-compartmentalized stacks, so that the total area remains the same in all configurations.

The costs for the energy storage are based on the costs of the electrolyte C_E, costs for the tanks C_{Tank}, costs for the tubing C_{Tubes}, costs for heat exchangers C_{HE} and costs for pumps C_{Pump}. The component-costs depend on the specific component prices p (given in Table 2 in the Appendix) and scaling factors (see also equations (20) - (26) in the Appendix). The costs for electrolyte and tanks both depend on the required electrolyte volume. Volume flow and size of heat exchangers is chosen according to the value given by Minke[12] or extrapolated according to the linear relations. Length of the tubing is calculated according to the number of stacks. The assembly of the energy storage accounts for 20% of the total costs for the energy storage.

3.1.1 Electrolyte Volume

In order to calculate the investment costs for the energy storage, it is important to know the necessary electrolyte volume. For the state of the art configuration, the total electrolyte volume $V_{\mathrm{E,ref}}$ and the depending total tank volume is given by[12]. The electrolyte volumes of the herein introduced configurations differ due to two effects: (i) A change in roundtrip efficiency results in electrolyte volume change $V_{\mathrm{E,CON},\varepsilon}$ via (10). (ii) A wider DOD allows the use of electrolyte more efficiently, thus allowing to reduce the amount of electrolyte needed by $V_{\mathrm{E,CON,DOD}}$ via (11). The resulting electrolyte volume $V_{\mathrm{E,CON}}$ of configuration

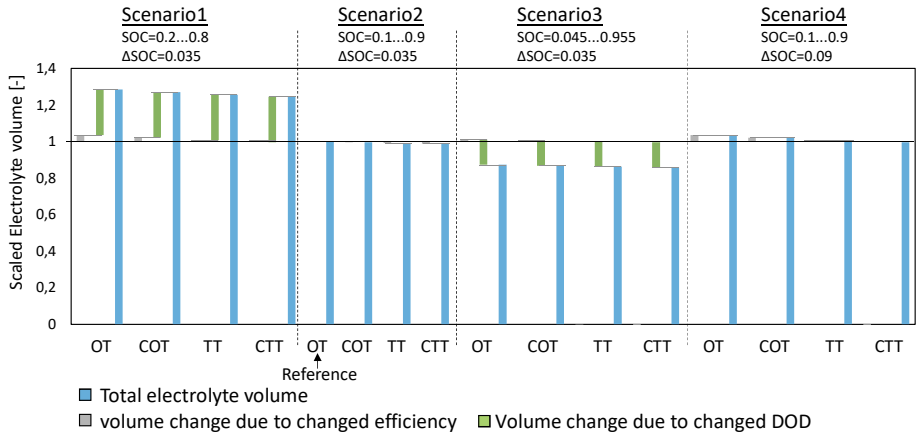

Fig. 7: Electrolyte Volume of each configuration for $j = 200\text{mA/cm}^2$ in each Scenario.

CON is calculated via (12).

$$V_{\text{E,CON},\varepsilon} = V_{\text{E,ref}} \cdot \Delta\varepsilon_{\text{ref}} \tag{10}$$

$$V_{\text{E,CON,DOD}} = V_{\text{E,ref}} \cdot \frac{\text{DOD}_{ref}}{\text{DOD}_{\text{CON}}} \tag{11}$$

$$V_{\text{E,CON}} = V_{\text{E,ref}} - V_{\text{E,CON},\varepsilon} - V_{\text{E,CON,DOD}} \tag{12}$$

The changing volumes for the analyzed configurations and the resulting total electrolyte volumes are shown in Figure 7. $V_{\text{E,CON,DOD}}$ (shown in green) is the same for all configurations in each Scenario 1, 2, 3 and 4, respectively, as the DOD is the same within each Scenario for all configurations. The narrow DOD in Scenario 1 results in electrolyte volume increase compared to the reference case, whereas the volume is decreased in Scenario 3. The decrease in roundtrip efficiency of OT and COT increase the total electrolyte demand in Scenario 4. The CTT configuration results in the lowest required amount of electrolyte in each scenario. A reduction of required electrolyte leads to lower investment costs for the electrolyte. The tank costs are based on the required tank volume.

3.1.2 Tank Cost Calculation

In the OneTank (OT and COT) configurations, tank volumes are equal to the electrolyte volume whereas for the TwoTank configurations (TT and CTT), the total tank volume is higher due to the extra storage tank per halfcell. Considering a VRFB consisting of only one tank per halfcell requires the installation of an additional tank per halfcell of the same size to fit the whole electrolyte. However, Figure 8 (left) illustrates that even in the OT configuration industrial plants at large scale often have several tanks per halfcell instead of one large tank. The electrolyte is nevertheless mixed simultaneously in all tanks together (so that the total volume of electrolyte has the same concentration in all small tanks). A flow strategy in which each small tank is now filled and emptied one after the other, as shown for the right halfcell, can result in requiring only a single additional tank to implement the TwoTank configuration instead of having to double the total tank volume. This would result in only marginally higher investment costs of one tank, but the higher roundtrip efficiencies of the TwoTank configurations can be achieved resulting in lower total costs. The naming "OneTank" and "TwoTank" thus is not entirely consistent with the number of tanks in real systems, however, it supports the basic distinction into configurations where the whole tank content is mixed at all times (OneTank) and configurations where the electroyte at different SOCs is stored separately (TwoTank). In the following cost calculations we therefore give upper and lower bounds for the investment costs and total costs to capture the maximal costs which are incurred when the tank volume has to be doubled. We also consider the minimal investment costs assuming that many small tanks are built and that the additional investment costs due to an additional tank are negligible.

3.2 Energy Cost Calculation

We keep the amount of released energy of discharge from the VRFB W_{out} fixed within DOD. Furthermore, we assume that the stored electricity is sold to the

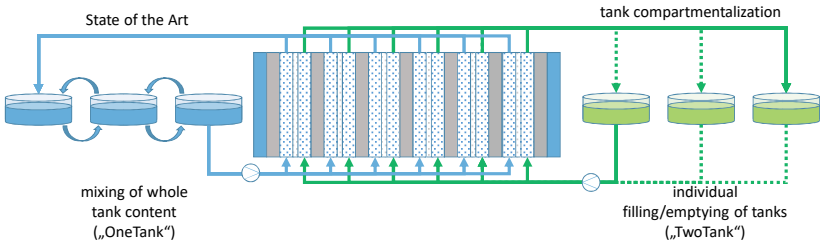

Fig. 8: Adjustment of the tank filling and mixing to reach the twotank configuration via compartmentalization of the tanks.

grid with the same duration of discharge and at the same time for each configuration, i.e., at the same electricity price on the electricity market. This implies the same earnings for electricity with each configuration. The energy costs for charging, however, will be different due to the different roundtrip efficiencies for reaching the fixed W_{out}. We keep electricity output fixed among all configurations and thus, the earnings due to selling W_{out} will be the same. Therefore, it is economically beneficial to chose the configuration with the lowest total costs where the total investment costs and the electricity costs for W_{in} are considered respectively for each configuration.

Number of cycles over the batteries lifetime are given in the order of 5,000-14,000[6] or 10,000-15,000[7] cycles per lifetime. Herein, we calculate with 10,000 cycles per lifetime. Considering a longer lifetime or equivalently a higher number of cycles per lifetime, an increase in efficiency will be even more advantageous, as energy costs will have a greater impact on total costs. This will argue in favor of the newly proposed configurations. With the given energy output W_{out} and efficiency of each configuration we can calculate the electricity need over the lifetime, assuming operation only with full cycles of analyzed DOD. Multiplied with an average electricity price, we can calculate the electricity costs for battery charging. Note that the electricity price will change in the future, but the change and the values are uncertain. In this study, we consider the average electricity price of the German EPEX SPOT in 2018 of $44\frac{€}{\text{MWh}}$[1].

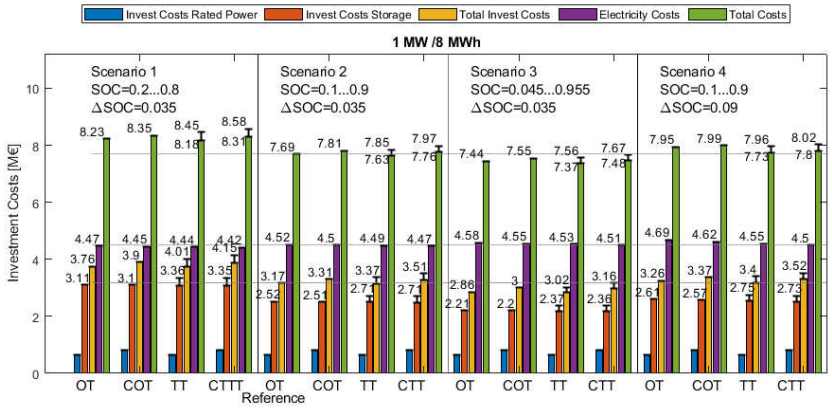

Fig. 9: Results of investment costs calculation for $j = 200\text{mA/cm}^2$ of each configuration at 1MW - 8MWh in each Scenario. Uncertainty in investment costs for tanks result in uncertainty of investment costs for rated power, total investment costs and total costs and are indicated by the black bar-lines (The numbers are given for maximal values).

3.3 Results of Cost Calculation

The techno-economic model in Minke[12] is based on linear relations of total costs, size of the electrochemical cell, storage capacity and specific material costs. Minke established the model for systems with rated power in the range 1-20 MW and energy storage in the range of 4MWh-160MWh. We implemented the model in MATLAB and applied it to a VRFB with 1MW/8MWh and to a system with 100 MW rated power and 8h of storage, i.e., 100MW/800MWh. According to Minke[12], the small RFB (1MW/8MWh) in state of the art configuration (OT) is equipped with one stack per halfcell. Therefore, dividing the single stack for compartmentalization into two compartments for COT and CTT results in four stacks and incurs further investment costs. RFBs with higher rated power are built with more than one stack per halfcell anyway according to Minke[12]. Compartmentalization in the large system (100MW/800MWh) can therefore be realized if stacks are connected in series. This would require a different laying of the tubes, but no additional investment costs for compartmentalization.

Figures 9 and 10 present the results of the total cost calculations for the small and large scale system, respectively.

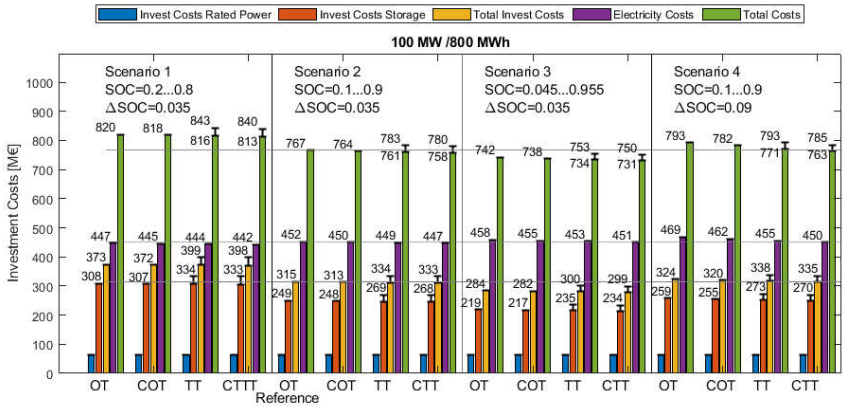

Fig. 10: Results of investment costs calculation for $j = 200\text{mA/cm}^2$ of each configuration at 100MW - 800MWh in each Scenario. Uncertainty in investment costs for tanks result in uncertainty of investment costs for rated power, total investment costs and total costs and are indicated by the black bar-lines (The numbers are given for maximal values).

Equipping the state of the art configuration with additional compartments increases the investment costs for rated power for the 1MW/8MWh system significantly due to the significantly higher number of stacks (doubled). Non-compartmentalized configurations need an investment of 0.65M€, whereas the configurations with 2 compartments have an investment for rated power of 0.8M€ for 1MW of rated power. This corresponds to an increase of 23%. In the large system (100MW/800MWh), we assume that compartmentalization may be achieved by connecting the stacks in series, therefore, the investment costs for rated power are the same for each configuration and each scenario. According to our calculations and according to Minke[12], the investment costs related to rated power are about 22% of the total investment costs in the reference case. A change in the stack costs in the small scale VRFB, therefore only accounts for higher total investment costs of ∼7% of COT compared to OT in Scenario 2. As the roundtrip efficiency was not increased significantly, the total costs are higher than for OT in the small scale VRFB. In the large scale battery, the slightly higher roundtrip efficiency reduces the total investment costs of COT compared to OT in all scenarios (up to 1.2% in Scenario 4) due to lower need

of electrolyte.

The design change of OneTank towards a TwoTank configuration leads to increased investment costs for tanks. At the same time, the higher efficiency enables the necessary electrolyte volume to be reduced and thus investment costs to be reduced. As stated in Section 3.1.2, we calculate the range of minimal and maximal investment costs for the additional tanks. The storage investment costs for the OneTank configurations and minimal costs for the TwoTank configuration are very similar in each scenario. The respective differences only occur due to roundtrip efficiency differences. The maximal storage investment costs for the TwoTank configurations are higher by ∼8% than the minimal investment costs for storage. Comparing the investment costs for storage in different scenarios reveals that increasing DOD results in significant investment reductions, e.g., from 2.52M€ for OT of the small VRFB in Scenario 2 (reference of the small VRFB) to 2.21M€ for OT in Scenario 3 which is a reduction by ∼12%.

The lowest total costs of the small scale VRFB are achieved with the OT configuration in Scenario 3, i.e., with a broad DOD of 4.5...95.5% and ΔSOC=3.5%. In all scenarios with a small ΔSOC, i.e., Scenario 1, 2 and 3, the configurations can be ranked according to their total costs in the same ascending order for the small scale VRFB: OT<TT<COT<CTT. This implies that additional investment costs are economically not advantageous for the small VRFB with the current cost structure. The increase in capital costs outweighs the increase in roundtrip efficiency.

For the large scale VRFB, the lowest total costs are achieved with the COT configuration in Scenario 3 if tank costs are assumed to be at their maximum. Assuming minimal tank costs, the CTT configuration of the same scenario results in the lowest total costs. In all scenarios with a small ΔSOC, i.e., Scenario 1, 2 and 3, the configurations can be ranked according to their total costs in the same ascending order (different to the small scale VRFB): COT<OT<CTT<TT. If higher ΔSOC's are required as in Scenario 4, the CTT configuration results in the lowest total costs if minimal tank costs are

assumed (lower than OT configuration by 3.7%) - COT if maximal tank costs are assumed (lower than OT configuration by 1.3%).

In both, the small scale and the large scale VRFB, the herein proposed modifications result in higher roundtrip efficiencies which leads to savings in electricity costs. If future electricity prices rise due to an increase in the use of renewable energy sources for electricity provision, the impact of electricity savings will increase and the proposed configurations may turn economical or have an even higher impact on total cost savings.

4 Conclusion

This manuscript highlights loss terms in a VRFB that are related to electrolyte mixing in a single electrolyte tank and a spatially uniform voltage along the flow direction in the electrical cell. Means to overcome these losses are discussed and evaluated based on a state of the art VRFB. In order to overcome these losses, we propose novel designs and operation strategies for redox flow batteries. The suggested designs include the addition of electrolyte tanks and the division of the electrochemical cells into compartments. Roundtrip efficiencies are evaluated based on charge and discharge curves for different current densities. Both proposed modifications and their combination result in higher roundtrip efficiencies revealing the reduction of losses. The efficiency increase due to compartmentalization is minor compared to the avoidance of mixing. For commonly applied operating strategies, the novel designs result in slightly lower use of electrolyte and marginally higher roundtrip efficiencies. If the change in SOC per pass through the cell is increased, the novel designs save a little more electrolyte and result in higher roundtrip efficiencies (up to 4%). Increased roundtrip efficiencies lead to operating cost reductions. However, the implementation of the designs require additional capital investments. The savings in the operating costs and the additional investment costs must be regarded simultaneously and are therefore considered cumulatively as total costs. Considering

a VRFB consisting of only one stack and of only one tank per halfcell, the investment costs for additional stacks and additional tanks are very high. Then, the state of the art configuration is economically the most beneficial for typical operating scenarios. If higher per pass changes are required, the total costs are lowest for a configuration with two tanks per halfcell. Large scale VRFBs are typically built with several stacks and tanks per halfcell anyway. This reduces the additional investment costs and therefore may result in higher total cost savings. Depending on the costs for storage, the total costs may be reduced by 1.3% or even 3.7% compared to the state of the art.

All in all, the total cost reductions seem small or only economical under certain limitations. However, this manuscript points out two important causes for efficiency losses and therefore aims at encouraging to consider if compartmentalization and TwoTank configuration may be implemented when designing a VRFB. We showed ways of taking both causes of losses into account when designing a VRFB. Other options to avoid these losses are conceivable and should also be included in future considerations. Stratification of the concentration in a single tank may be a difficult approach to implement, but it may avoid mixing and thus the losses induced by it.

The effect of the simultaneous increase of efficiency and decrease in electrolyte requirement in ecological metrics may be higher than in economic metrics. Thus, it is advisable to also perform an LCA analysis.

Furthermore, temperature management is important for the safe and efficient operation of an RFB. It is expected that the proposed design changes will have no significant impact on this issue if only additional tanks are introduced as in the TT configuration. However, if existing stacks are to be connected in series to implement the compartmentalized configuration, the temperature change of the electrolyte may be too high and needs to be investigated in detail. Additionally, especially for Scenario 3 which goes beyond typical limits in SOC, temperature management and investment costs for non-aqueous electrolytes should be examined.

Future investigations should also validate the considered lumped ohmic resistance and the resulting voltage curves over the SOC range. Alternatively, the underlying phenomena such as mass transport could be modeled in detail.

Acknowledgement

The authors gratefully acknowledge the financial support of the Kopernikus Project SynErgie by the Federal Ministry of Education and Research (BMBF) and the project supervision by the project management organization Projektträger Jülich (PtJ). We would like to thank Kosan Roh and Jonas Kuhlmann for starting to look into flow batteries and thus inspiring us. We would also like to thank Deniz Rall and Korcan Percin for valuable discussions and input.

References

[1] Agora Energiewende, 2019.

[2] M. Akter, Y. Li, J. Bao, M. Skyllas-Kazacos, and M. Rahman. Optimal Charging of Vanadium Redox Flow Battery with Time-Varying Input Power. *Batteries*, 5(1):20, 2019.

[3] P. Alotto, M. Guarnieri, and F. Moro. Redox flow batteries for the storage of renewable energy: A review. *Renewable and Sustainable Energy Reviews*, 29:325–335, 2014.

[4] T. Bauer. Energie aus dem Salz, Hochtemperatur-Wärmespeicherung in Flüssigsalzspeichern. *BWK Das Energie-Fachmagazin*, (5):42–44, 2019.

[5] C. Blanc and A. Rufer. Understanding the Vanadium Redox Flow Batteries: 18. In J. Nathwani and A. Ng, editors, *Paths to Sustainable Energy*. IntechOpen, Rijeka, 2010.

[6] M. H. Chakrabarti, F. S. Mjalli, I. M. AlNashef, M. A. Hashim, M. A. Hussain, L. Bahadori, and C. T. J. Low. Prospects of applying ionic liquids

and deep eutectic solvents for renewable energy storage by means of redox flow batteries. *Renewable and Sustainable Energy Reviews*, 30:254–270, 2014.

[7] S. Eckroad. Vanadium redox flow batteries: an in-depth analysis. *Electric Power Research Institute, Palo Alto, CA*, 1014836, 2007.

[8] T. Herr, P. Fischer, J. Tübke, K. Pinkwart, and P. Elsner. Increasing the energy density of the non-aqueous vanadium redox flow battery with the acetonitrile-1,3-dioxolane–dimethyl sulfoxide solvent mixture. *Journal of Power Sources*, 265:317–324, 2014.

[9] S. Kim. Vanadium Redox Flow Batteries: Electrochemical Engineering. In T. Damirkan and A. Attia, editors, *Energy Storage Devices*. 2019.

[10] B. Liu, M. Zheng, J. Sun, and Z. Yu. No-mixing design of vanadium redox flow battery for enhanced effective energy capacity. *Journal of Energy Storage*, 23:278–291, 2019.

[11] E. Lizarraga-Garcia, A. Ghobeity, M. Totten, and A. Mitsos. Optimal operation of a solar-thermal power plant with energy storage and electricity buy-back from grid. *Energy*, 51:61–70, 2013.

[12] C. Minke. *Techno-ökonomische Modellierung und Bewertung von stationären Vanadium-Redox-Flow-Batterien im industriellen Maßstab*, volume v.40 of *Schriftenreihe des Energie-Forschungszentrums Niedersachsen (EFZN)*. Cuvillier Verlag, Göttingen, 1st ed. edition, 2016.

[13] J. S. Newman and K. E. Thomas-Alyea. *Electrochemical systems: Third Edition*. J. Wiley, Hoboken and N.J, 3 edition, 2004.

[14] J. D. Osorio, R. Hovsapian, and J. C. Ordonez. Effect of multi-tank thermal energy storage, recuperator effectiveness, and solar receiver conductance on the performance of a concentrated solar supercritical CO2-based power

plant operating under different seasonal conditions. *Energy*, 115:353–368, 2016.

[15] F. Pan and Q. Wang. Redox Species of Redox Flow Batteries: A Review. *Molecules*, 20(11):20499–20517, 2015.

[16] A. Parasuraman, T. M. Lim, C. Menictas, and M. Skyllas-Kazacos. Review of material research and development for vanadium redox flow battery applications. *Electrochimica Acta*, 101:27–40, 2013.

[17] A. A. Shinkle, A. E. S. Sleightholme, L. T. Thompson, and C. W. Monroe. Electrode kinetics in non-aqueous vanadium acetylacetonate redox flow batteries. *Journal of Applied Electrochemistry*, 41(10):1191–1199, 2011.

[18] A. Tang, J. Bao, and M. Skyllas-Kazacos. Dynamic modelling of the effects of ion diffusion and side reactions on the capacity loss for vanadium redox flow battery. *Journal of Power Sources*, 196(24):10737–10747, 2011.

[19] V. Viswanathan, A. Crawford, D. Stephenson, S. Kim, W. Wang, B. Li, G. Coffey, E. Thomsen, G. Graff, P. Balducci, M. Kintner-Meyer, and V. Sprenkle. Cost and performance model for redox flow batteries. *Journal of Power Sources*, 247:1040–1051, 2014.

[20] J. F. Weaver. World's largest battery: 200MW/800MWh vanadium flow battery - site work ongoing; last accessed: 2019 Aug. 9th, 2017.

[21] Z. Wei, T. M. Lim, M. Skyllas-Kazacos, N. Wai, and K. J. Tseng. Online state of charge and model parameter co-estimation based on a novel multi-timescale estimator for vanadium redox flow battery. *Applied Energy*, 172:169–179, 2016.

[22] Z. Wei, K. J. Tseng, N. Wai, T. M. Lim, and M. Skyllas-Kazacos. Adaptive estimation of state of charge and capacity with online identified battery model for vanadium redox flow battery. *Journal of Power Sources*, 332:389–398, 2016.

[23] Z. Wei, J. Zhao, and B. Xiong. Dynamic electro-thermal modeling of all-vanadium redox flow battery with forced cooling strategies. *Applied Energy*, 135:1–10, 2014.

[24] W. Weydanz and A. Jossen. *Moderne Akkumulatoren richtig einsetzen*. Ubooks-Verlag, Neusäß, 2006.

Appendix

Investment Cost calculation according to Minke[12]

Stackcosts per stack:

$$C_{Stack} = C_M + C_{Electrode} + C_{BPP} + C_{CC} + C_{CF} + C_F + C_{RP,Assembly} \quad (13)$$

$$C_M = A_C \cdot n_{Cells} \cdot p_M \quad (14)$$

$$C_{Electrode} = A_C \cdot n_{Cells} \cdot 2 \cdot p_{Electrode} \quad (15)$$

$$C_{BPP} = A_C \cdot (n_{Cells} + 1) \cdot p_{BPP} \quad (16)$$

$$C_{CC} = 2 \cdot p_{CC} \quad (17)$$

$$C_{CF} = n_{Cells} \cdot p_{CF} \quad (18)$$

Connection costs of the stacks for the whole VRFB: (Note that apparently the presented results in Minke[12] are based on assuming that $p_{PLS,1}$=0, underestimating the cost of the control system by a factor of 3 for the assumed 1MW production rate. For 100MW the difference is negligible.)

$$C_C = (p_{conv} + p_{cab} + p_{PLS,2}) \cdot P_{VRFB} + p_{PLS,1} \quad (19)$$

costs for energy storage of the VRFB:

$$C_{storage} = C_E + C_{Tank} + C_{Pump} + C_{Tubes} + C_{HE} + C_{S,Assembly} \quad (20)$$

$$C_{E/Tank} = V_{E/Tank} \cdot p_{E/Tank} \quad (21)$$

$$C_{Pump} = 2 \cdot n_{halfcells} \cdot V_E \cdot p_{Pump} \quad (22)$$

$$C_{Tubes} = l_{Tubes} \cdot p_{Tubes} \quad (23)$$

$$l_{Tubes} = n_{halfcells} \cdot (30m + n_{Stacks} \cdot 5m) \quad (24)$$

$$C_{HE} = A_{HE} \cdot p_{HE} \quad (25)$$

$$C_{S,Assembly} = 20\% \text{ of } C_{storage} \quad (26)$$

Table 2: Specific costs taken from Minke[12]

component	symbol	specific costs
costs related to rated power		
stack costs		
membrane [€/m^2]	p_M	400
electrode [€/m^2]	$p_{Electrode}$	60
BPP [€/m^2]	p_{BPP}	200
current collector [€/piece]	p_{CC}	3,000
cell framing [€/piece]	p_{CF}	200
stack framing [€/piece]	C_{ST}	25,000
stack assembly [€/piece]	$C_{RP,Assembly}$	27,500
connection costs		
converter [€/MW]	p_{conv}	100,000
cabling [€/MW]	p_{cab}	2,000
process control system	$p_{PLS,1}$	50,000 €/piece +
	$p_{PLS,2}$	100,000 €/MW
costs related to energy storage		
electrolyte [€/m^3]	p_E	4,500
tanks [€/m^3]	p_{Tank}	300
pumps [€/(m^3/h)]	p_{Pump}	64
tubing [€/m]	p_{Tubes}	600
heat exchangers [€/m^2]	p_{HE}	180
assembly [% of energy invest]	$p_{S,Assembly}$	20

Table 3: Settings for the configurations in the cost calculation.

	OT*	COT	TT	CTT
1MW - 8MWh				
rated power [MW]	1	1	1	1
energy output at discharge [MWh]	8	8	8	8
cell area [m^2]	2.7	1.35	2.7	1.35
cells per stack	78	78	78	78
number of stacks	2	4	2	4
length of tubing [m]	60	100	60	100
area heat exchangers [m^2]	54	54	54	54
100MW - 800MWh				
rated power [MW]	100	100	100	100
energy output at discharge [MWh]	800	800	800	800
cell area [m^2]	2.7	1.35	2.7	1.35
cells per stack	78	78	78	78
number of stacks	200	200	200	200
length of tubing [m]	1060	1060	1060	1060
area heat exchangers [m^2]	5,373	5,373	5,373	5,373

*values for OT are taken from Minke[12]